

# Victims of ancient hyperthermal events herald the fates of marine clades and traits under global warming

Carl J. Reddin<sup>1,2</sup>  | *Ádám T. Kocsis*<sup>1,3</sup>  | Martin Aberhan<sup>2</sup>  | Wolfgang Kiessling<sup>1</sup> 

<sup>1</sup>GeoZentrum Nordbayern, Friedrich-Alexander-University Erlangen-Nürnberg, Erlangen, Germany

<sup>2</sup>Museum für Naturkunde, Leibniz Institute for Evolution and Biodiversity Science, Berlin, Germany

<sup>3</sup>MTA-MTM-ELTE Research Group for Paleontology, Budapest, Hungary

## Correspondence

Carl J. Reddin, Museum für Naturkunde, Leibniz Institute for Evolution and Biodiversity Science, Invalidenstraße 43, 10115 Berlin, Germany.  
Email: carl.reddin@mf.n.berlin

## Funding information

Deutsche Forschungsgemeinschaft, Grant/Award Number: AB 109/11-1, KI 806/16-1 and KO 5382/2-1; Volkswagen Foundation

## Abstract

Organismic groups vary non-randomly in their vulnerability to extinction. However, it is unclear whether the same groups are consistently vulnerable, regardless of the dominant extinction drivers, or whether certain drivers have their own distinctive and predictable victims. Given the challenges presented by anthropogenic global warming, we focus on changes in extinction selectivity trends during ancient hyperthermal events: geologically rapid episodes of global warming. Focusing on the fossil record of the last 300 million years, we identify clades and traits of marine ectotherms that were more prone to extinction under the onset of six hyperthermal events than during other times. Hyperthermals enhanced the vulnerability of marine fauna that host photosymbionts, particularly zooxanthellate corals, the reef environments they provide, and genera with actively burrowing or swimming adult life-stages. The extinction risk of larger sized fauna also increased relative to non-hyperthermal times, while genera with a poorly buffered internal physiology did not become more vulnerable on average during hyperthermals. Hyperthermal-vulnerable clades include rhynchonelliform brachiopods and bony fish, whereas resistant clades include cartilaginous fish, and ostreid and venerid bivalves. These extinction responses in the geological past mirror modern responses of these groups to warming, including range-shift magnitudes, population losses, and experimental performance under climate-related stressors. Accordingly, extinction mechanisms distinctive to rapid global warming may be indicated, including sensitivity to warming-induced seawater deoxygenation. In anticipation of modern warming-driven marine extinctions, the trends illustrated in the fossil record offer an expedient preview.

## KEYWORDS

climate change, extinction, fossil, metabolic activity, photosymbiont, selectivity

## 1 | INTRODUCTION

Climate change is expected to push some groups of species closer to extinction while others may abide the change (Dunhill et al., 2018; Knoll et al., 2007; Reddin et al., 2020). Yet, modern

climate change-driven extinctions so far remain scarce or causally ambiguous (Cahill et al., 2013). This is partly because concurrent anthropogenic stressors, including habitat loss and overexploitation, obscure the prediction of which modern species are specifically at risk of climate change-driven extinction (Harnik et al., 2012). The

This is an open access article under the terms of the Creative Commons Attribution License, which permits use, distribution and reproduction in any medium, provided the original work is properly cited.

© 2020 The Authors. *Global Change Biology* published by John Wiley & Sons Ltd

deep-time fossil record, conversely, is free from human impacts, and documents extinctions during ancient episodes of rapid climate warming, or hyperthermals. Foster et al. (2018) described six global hyperthermal events that shared a rapid increase in tropical sea surface temperatures, generally greater than 2°C with an onset duration less than 100,000 years, widespread oceanic deoxygenation, intensifying hydrological cycles, and a doubling of atmospheric CO<sub>2</sub> that induces collateral ocean acidification. However, the equivalence between ancient biotic responses to hyperthermals and the biotic responses exhibited today is often questioned. Ancient hyperthermal events were initially triggered by volcanic degassing (Foster et al., 2018). Then, the proliferation of calcareous plankton, including coccolithophores and foraminifera, from the Middle Jurassic onward may have formed a game-changing buffer against rapid changes in ocean chemistry (Ridgwell, 2005). Notwithstanding such changes, consistent winners and losers of hyperthermals can emerge (Reddin et al., 2020).

Certain clades have long species durations, such as scleractinian corals, whereas others, such as ammonites, have a high evolutionary turnover (Finnegan et al., 2015; McKinney, 1997; Raup & Boyajian, 1988). One interpretation is “that the same groups are generally less susceptible to extinction from all possible causes” (McKinney, 1997). Accordingly, resistant groups should have a consistently low extinction selectivity: the extinction magnitude of a certain taxon or trait relative to the overall extinction magnitude, or to that of another group (Bush et al., 2020; Clapham, 2017; Clapham & Payne, 2011; Dunhill et al., 2018; Foote, 2006; Kiessling & Aberhan, 2007; McKinney, 1997; Nürnberg & Aberhan, 2015; Orzechowski et al., 2015; Payne & Heim, 2020). Alternatively, if particular stressors dominate an extinction event (and are less relevant at others), these may expose atypical vulnerabilities of particular taxa and traits. Hypotheses include that smaller rather than larger body sizes fare better under heat stress (Piazza et al., 2020), that infauna may be removed by seafloor anoxia (Aberhan & Baumiller, 2003), and that taxa with poor internal chemical buffering or large mass of exposed calcium carbonate relative to organic mass are unable to tolerate rapid changes in ocean chemistry (Bambach et al., 2002; Knoll et al., 2007). However, the different baseline turnover rates of different groups need accounting for to identify patterns unique to hyperthermals. Additionally, previous analyses have either focused on a single crisis or mix crises that vary by the dominant hypothesized extinction trigger(s). Under such conditions, a consistent mechanistic basis linking trigger and extinction cannot be truly tested.

Mechanisms that decrease population performance and fitness under climate-related stressors can be revealed, however, via controlled experiments with living organisms. Experiments demonstrate clear clade-level variation in performance responses (Harvey et al., 2013; Storch et al., 2014; Wittmann & Pörtner, 2013). Hypothesized mechanisms include differences in skeletal mineralogy and level of calcification (Harvey et al., 2013), and differences in respiratory physiology such as mass-specific aerobic scope (Bozinovic & Pörtner, 2015; Peck et al., 2009). Correlative evidence supports that such mechanisms

scale-up to risk of global extinction (Reddin et al., 2020). However, more work is needed to establish which groups are uniquely at risk of extinction under global warming, which is essential information for prediction and setting modern conservation priorities.

To test these hypotheses, we quantify hyperthermal vulnerability of marine metazoan ectotherm clades and traits over the past 300 million years using fossil occurrences from the Paleobiology Database (PaleoDB, <https://paleobiodb.org>). We contrast selectivity regimes during the onset of the six hyperthermal events identified by Foster et al. (2018) against those during non-hyperthermal geological ages. The difference of this average hyperthermal selectivity and the respective baseline selectivity quantifies how much more likely a taxon is to go extinct during a hyperthermal, based on its clade membership or trait, than it is under non-hyperthermal conditions. This difference, which we term relative hyperthermal vulnerability (RHV), places groups with high and low typical rates of turnover, for example, ammonites versus scleractinian corals, on an equal footing, and emphasizes patterns that are exclusive to hyperthermal events. Thus, RHV differs from the typical quantification of extinction selectivity (Bush et al., 2020; Orzechowski et al., 2015). Additionally, we evaluate the influence on RHV of one of the most relevant Earth system changes, the mid-Jurassic plankton revolution, which is thought to have ameliorated the impact of widespread abiotic change on organisms and ecosystems (Eichenseer et al., 2019; Ridgwell, 2005). We explicitly control for geographic range size and clade membership, which are among the strongest predictors of extinction risk through geological time (Finnegan et al., 2015).

## 2 | METHODS

### 2.1 | Hyperthermal events

We identify hyperthermal events over the last 300 million years (Permian to Neogene) following the evidence and criteria set by Foster et al. (2018). These events include the Permian–Triassic (PT, ~252 Ma), Triassic–Jurassic (TJ, ~201.3 Ma), the end-Pliensbachian–early Toarcian (Pli-Toa, ~183 Ma), the OAE1 (Aptian, ~120 Ma), the OAE2 (Cenomanian–Turonian, ~94 Ma), and the Paleocene–Eocene Thermal Maximum (PETM, ~55.5 Ma). They varied in their extinction toll from the greatest extinction of the Phanerozoic, the PT, along with the TJ mass extinction before the mid-Jurassic plankton revolution, to the “muted or mixed” (Foster et al., 2018) biotic responses thereafter. The most recent of these hyperthermals, the PETM, only caused considerable extinction among deep-sea foraminifera (Thomas, 2007). Our analytical resolution is at the level of chronostratigraphic stage, while the onset of hyperthermal conditions, which sometimes covered multiple stages, often occurred near but not precisely at stage boundaries. We chose to use the stage boundary that best separates genera last observed before the hyperthermal onset from those that survived after the onset, including the Changhsingian for the PT (Sun et al., 2012) and the Pliensbachian for

the Pli-Toa (Suan et al., 2010). Such hyperthermal onset extinctions are expected to be most relevant for anticipating modern extinctions, while extinctions from subsequent warming pulses, including the late Smithian and early Toarcian Oceanic Anoxic Event proper, occurred in an already hyperthermal-impacted world. Thus, we exclude the Induan, Olenekian, and Toarcian stages from our analyses. Following Foster et al. (2018), we do not consider orbitally forced, lower magnitude warming events of the Cenozoic.

## 2.2 | Data preparation

We downloaded data on post-Cambrian marine animal fossils from the publicly accessible PaleoDB (<https://paleobiodb.org/>) on 25 May 2020. Although the main analyses centered on the past 300 million years, data of earlier time intervals were used to calculate more accurate genus durations, survivals, and habitat affinities. We retained genus occurrences only from marine depositional settings and from marine ectotherm classes or phyla, omitting any uncertain classifications or genera unique to a single collection. These were then binned to chronostratigraphic stages following the standard steps in the “ddPhanero” vignette accompanying R package *divDyn* (Kocsis et al., 2019; <https://doi.org/10.5281/zenodo.2545983>), with unbinned occurrences removed. Extinction magnitude and sampling completeness were calculated by the “second-for-third” extinction rates of Alroy (2015) and the three-timer sampling completeness of Alroy (2008), respectively, using R package *divDyn* (Kocsis et al., 2019).

The clade levels used were based on the understanding of a group's ecological trait variation and the quality of their fossil record. Therefore, we used orders for bivalves and anthozoans, subclasses for cephalopods, subphyla for brachiopods and arthropods, and classes for all others. We assessed whether bivalve orders with fewer than 100 genera could be pooled to higher taxa that did meet the 100 genera threshold, without mixing trait characteristics within the clade. This resulted in Pholadomyida, Thraciida, Pandorida, and Poromyida being pooled into the Superorder Anomalodesmata. Some traits derive from the standard PaleoDB fields, including primary skeletal mineralogy, motility, life habit, and dietary traits, although the numerous entries were aggregated to a handful of traits (Table 1). Non-random affinities of genera (habitat preferences) either to siliciclastic or carbonate primary lithology, to offshore or nearshore depositional environments (often termed “deep” and “shallow,” respectively), or to reef or non-reef habitats were calculated using binomial tests and an alpha level  $\alpha = 0.1$  using the R package *divDyn* (Kiessling & Aberhan, 2007; Kocsis et al., 2019). The odds in the binomial tests were derived from the proportions of sampled environments. We also used the dataset of Payne and Heim (2020) with duplicates removed to assign body size (log-volume) data for genera, which was successful for 35% of our genera. Body size was thus a continuous variable. Finally, we tested the well-buffered and poorly buffered grouping scheme of Bambach et al. (2002). Some genera or traits had ecological information missing from the

**TABLE 1** The ecological trait groups and their levels, excluding the binary variables, that is, habitat preferences and buffering. For trait designation, the PaleoDB generally has a primary and secondary entry. Here, the primary entry took precedent, unless the secondary dietary entry was reliance on a symbiont (in which case “photosymbiotic” or “chemosymbiotic” became the designation) or the primary entry was a term not be easily categorized below

Trait group	Trait level	Treated as synonymous
Motility	Stationary	Attached
	Facultatively mobile	
	Passively mobile	Fast- or slow-moving <sup>a</sup>
	Actively mobile	
Primary skeletal mineralogy	High-Mg calcite	Intermediate (4%–10%) Mg calcite
	Low-Mg calcite	
	Aragonite	
	Silica	
	Phosphatic	
Life habit	Infaunal	Any depth
	Nektonic	Nektobenthic
	Planktonic	
	Epifaunal	Colonial, any tiering level
	Semi-infaunal	
Diet	Photosymbiotic	
	Chemosymbiotic	
	Suspension feeder	Microcarnivore
	Deposit feeder	Detritivore, coprophage
	Omnivore	Grazer, browser
	Carnivore	

<sup>a</sup>“Slow-moving” bivalves changed to “facultatively mobile.”

PaleoDB, so we used multivariate imputation by chained equations to populate a trait matrix of unduplicated genera using the R package *mice* (van Buuren & Groothuis-Oudshoorn, 2011). The chained equations used polytomous logistic regression for traits, using information from phylogeny (phylum, class, and clade, as above), the other traits (except habitat preferences, which were only available for common genera), and genus occupancy. We restricted imputation of missing values to the columns of skeletal mineralogy (93% of original genera complete), motility (99.9%), life habit (80%), diet (96%), and buffering (39%). Running analyses without trait imputation showed that imputation did not change the response ranking of RHV within ecological variables but did reduce errors (Figure S1). In particular, buffering had half of its values imputed based on genus clade membership and other ecological traits, but this imputation resembles how clades were originally categorized as poorly or well-buffered (Bambach et al., 2002), and the ordering of responses was not changed (Figure S1).

## 2.3 | Geographical range size

Range size has a known effect on extinction risk (Finnegan et al., 2015; Payne & Finnegan, 2007). We incorporated range size via two approaches and checked our results for consistency between them. These comprised using the genus occupancy of equal-area cells and the genus subsampled maximum great circle distance (GCD) as range size. Occupancy used equal-area hexagonal cells with a mean cell area of 794,000 km<sup>2</sup>, constructed using the R package *icosa* (Kocsis, 2020). Genus maximum GCD in a stage was calculated as the mean of 100 random subsamples of 600 occurrences. To avoid ranges of zero, we added +1 to all means. Because range-through interpolations were not represented by an empirical occurrence, these were assigned an arbitrary lowest value for range size (or occupancy) of 0.5. Both maximum GCD and occupancy were strongly skewed variables, which are likely to have adverse effects on the performance of regression models. To address this concern, genus maximum GCD were binned into an ordinal variable around the GCD quantiles per stage.  $Q_1$  and  $Q_2$  were fixed to avoid their overlap in a few stages:  $GCD_{bin1} = 0.5$ ,  $GCD_{bin2} = 1$ ,  $1 < GCD_{bin3} \leq Q_3$ ,  $GCD_{bin4} > Q_3$ . The ranking of traits and clades by RHV remained relatively consistent regardless of the range size treatment. This also applies when range size was not included in models, but we used binned GCD in models because of the important influence of range size on extinction risk (Finnegan et al., 2015; Payne & Finnegan, 2007). Latitudinal range size, by more closely representing thermal range, might arguably be more relevant during hyperthermal events. However, a large longitudinal range may also protect against extinction (both during non-hyperthermal and hyperthermal times). Geographical and latitudinal range nevertheless overlap and thus are very strongly correlated (Spearman's  $\rho = 0.93$ ,  $p < .0001$ ). This correlation included each genus once only, by calculating the geographic and latitudinal ranges of each genus per stage and using only the maximum value.

## 2.4 | Extinction selectivity models

After data preparation and calculations of habitat affinities and subsampled geographical range sizes, the analytical pipeline involved two main steps: (1) logistic mixed-effect regression models for each trait group (e.g., life habit) and clades, per stage; and (2) synthesizing the outputs of these stage-models in inverse-variance weighted, mixed-effect meta-regression for each trait or clade level separately (Reddin et al., 2020), once for hyperthermal stages and once for non-hyperthermal stages. Step (1) took the form of the R expression,

```
glmer(ext ~ diet + (diet|clade) + geog_range, family = "binomial")
```

using diet as the example trait group, with potential trait levels: Photosymbiotic, Chemosymbiotic, Suspension feeder, Deposit feeder, Omnivore, Carnivore. *ext* is the extinction response of each genus. *geog\_range* is geographical range via maximum GCD, as described above. *glmer* is the function in R package *lme4* (Bates et al., 2015). We used logistic regression to calculate extinction selectivity for each

post-Carboniferous stage, as genus extinction or survival predicted by clade or trait membership. We are interested in the effect of adult traits across different clades so included "clade" as a random effect in trait models, for example, denoted (diet|clade) above (except buffering, which was largely based on clade). Model fixed effects, for example, diet levels, were calculated relative to zero rather than to the model intercept and were then converted to extinction selectivity in the synthesis model.

To accommodate the potential effects of sampling heterogeneities on our results, we contrast three approaches, assuming varying confidence in the extinction or survival values. The first approach, (a) takes genus survival or extinction per geological stage at face value. In the second approach, (b) genus survival was interpolated between first and last observed occurrences since the Ordovician ("range-through", RT), lessening apparent extinction selectivity (by retaining unobserved survivals) of poorly sampled groups on average (Tables S1 and S2; Figure S2), and during poorly sampled stages (Figure S3). However, no geological stage represents perfect sampling so, although the "last appearance datum" (LAD) represents a true occurrence, it is unlikely to be the true last occurrence of a genus, potentially underestimating the age of extinction in (a) and (b). To reflect this uncertainty, (c) the binary extinction value, 1, was substituted with a sampling completeness value as an extinction probability in the last stage of occurrence. In this probabilistic approach, we averaged the three-timer sampling completeness (Alroy, 2008) of the following stage (i.e., the probability that if the genus survived into stage  $i + 1$  that it would have been sampled) and the Phanerozoic median sampling completeness of the group (clade or trait, Figures S2 and S3), because some clades are systematically better preserved than others (Foote & Raup, 1996). The remainder of the genus extinction probability ( $1 - \text{integrated sampling completeness value}^{i+1}$ ) represents the likelihood that the true genus last occurrence was actually in stage  $i + 1$ , but went unobserved, so this probability is passed onto the selectivity model for the following stage. The three methodological approaches are compared in the Supporting Information. To avoid small sample sizes, clades required a minimum of five genera to be included in any logistic regression model (also Bush et al., 2020), since this is the minimum  $n$  needed to be significant in a balanced binomial test ( $p < .1$ ).

## 2.5 | Synthesizing RHV

We wish to contrast extinction selectivity effect size and variance over stages that fit certain conditions, that is, onset of hyperthermal events versus non-hyperthermal times. To do this, the above model outputs for each geological stage from step (1) were passed to step (2), which was expressed in R as,

```
rma(stage_coefficients, mods = ~ext_rate).
```

This denotes an inverse-variance weighted synthesis meta-regression, one per trait or clade, which used a restricted maximum-likelihood

estimator. The data here are geological stages, treated as a random factor, using the factor coefficient, *stage\_coefficients* above, and its standard error, for example, for the dietary trait “carnivore.” *rma* is the function in R package *metafor* (Viechtbauer, 2010). To convert differences in extinction magnitude into differences in selectivity, we included overall extinction magnitude as a moderator,  $\text{mods} = \sim \text{ext\_rate}$  above, with different slopes allowed for different traits or clades.

This synthesis approach allows the separation of variances within and among stages, since their respective models were unbalanced in terms of number of occurrences, availability of traits, and sampling conditions. Meta-regressions synthesized the results for hyperthermal onset and non-hyperthermal stages separately, and the difference between the two, the RHV, was calculated by subtraction. RHV inherited error values from the hyperthermal synthesis meta-regression, which, being synthesized over fewer stages, always had larger error than the non-hyperthermal meta-regression. Traits or clades required a minimum representation of two hyperthermals. Despite the often low PETM RHV values, our metric for synthesized extinction selectivity and thus for RHV is independent of extinction magnitude (e.g., strongest time-series correlation between median selectivity and extinction magnitude was for clades,  $\rho = 0.16$ ,  $p = .26$ ). However, selectivity error was moderate-to-strongly correlated with extinction magnitude (e.g., strongest correlation between the median of selectivity SEs and extinction magnitude was for clades,  $\rho = -0.69$ ,  $p < .0001$ ). Stage model estimate error was used to weight the synthesis meta-regression, so that precise estimates contribute more to our analysis. Accordingly, this also meant that stages with higher extinction magnitudes had a higher influence on our analyses, while estimates for low extinction magnitude stages, which are susceptible to random error (Bush et al., 2020), contribute less. This may be unavoidable because, theoretically, maximum information entropy (here, selectivity signal) is possible when 50% of genera go extinct. However, 75% of stages have extinction magnitudes below 0.23, placing higher extinction magnitude stages closer to the theoretical point of maximum entropy than lower ones. The closest to this value was the non-hyperthermal K-T mass extinction (magnitude = 0.48), which consequently should have a stronger influence on non-hyperthermal selectivity than other non-hyperthermal stages. Nevertheless, exclusion of the K-T mass extinction from analysis does not affect the ranking of responses (Figure S4).

Analytical emphasis on uncertainty (i.e., using the hyperthermal errors for RHV), an expectation of high response variability within trait or clade levels, and only six hyperthermals to average over means the risk of type 2 statistical error was deemed high, so we report results at  $p < .1$  and use 90% rather than 95% CIs throughout.

Clades that are evenly spread over a range of traits may reduce phylogenetic overprinting of ecological patterns. Thus, we also compared responses among scleractinian dietary traits, and bivalve motility, life habit, and body sizes.

## 2.6 | Middle-Jurassic plankton revolution

Considering only the model outputs for hyperthermal stages, a synthesis model was used to estimate the effect of the Jurassic plankton revolution on the extinction selectivity per trait or clade. This was modeled by a simple binary predictor of hyperthermals before (PT, TJ, and Pli-Toa) and after the revolution (OAE1, OAE2, PETM), accounting for extinction magnitude and requiring a group to have at least two stage estimates before and two after the revolution. For comparison, we use a second synthesis model that was identical except that it did not contain a term for extinction magnitude, thus calculating the effect of the revolution on the extinction magnitude per trait or clade, that is, which groups drove the decrease in overall extinction magnitude.

## 3 | RESULTS

### 3.1 | Clades

Rhynchonelliform brachiopods, trioniid bivalves, and echinoids had the highest RHV (Figure 1; Table S3). Translated into probabilities, these genera have a 63% (90% CIs = 44%–79%), 70% (48%–86%), and 62% (45%–77%) chance of raised extinction risk during a hyperthermal than under non-hyperthermal conditions, although the exact increase in extinction risk depends on the group's non-hyperthermal baseline risk (see Figure S5). Consistent RHV trends across different treatments of sampling incompleteness also include high RHV for ammonoids, despite high baseline extinction odds (Figure S5), and negative RHV, indicating tolerance of hyperthermal conditions, for ostreid and venerid bivalves. A higher RHV of bony fishes than the more tolerant cartilaginous fishes gives a 68% chance of raised extinction risk for an Actinopterygii genus (CIs = 52%–80%; Figure 1) over a Chondrichthyes genus, which suggests bony fishes to be more uniquely vulnerable to hyperthermal conditions.

### 3.2 | Diet

With confidence intervals not overlapping zero, the point of no difference from non-hyperthermal extinction odds, the clearest RHV was for animals hosting photosymbionts, giving a genus 76% chance of raised extinction risk during a hyperthermal (CIs = 54%–89%; Figures 1 and 2a). Photosymbiotic animals were dominated by scleractinian corals (70%). Within this clade, zooxanthellate corals showed a significantly higher RHV than azooxanthellate corals, which had a large variance (Figure 3) and suppressed the overall scleractinian RHV (Figure 1). This difference among scleractinians is maintained during the PETM, which had a very low extinction magnitude and the highest RHV for deposit feeders (Figure 2a). Otherwise, suspension feeding was the most hyperthermal-resistant dietary trait (Figure 2a).



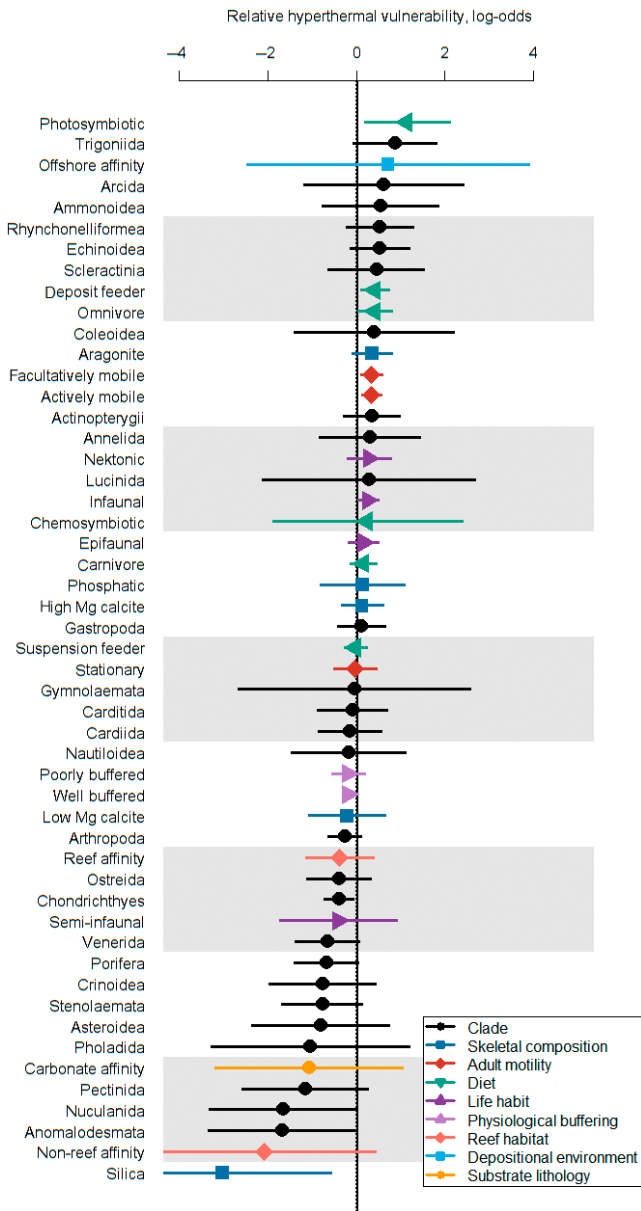


**FIGURE 1** Clades and traits ranked by relative hyperthermal vulnerability (RHV), the average increased risk of a genus to global warming. RHV is calculated relative to a non-hyperthermal baseline extinction risk for each trait or clade, so that zero means hyperthermal extinction risk is on average no different than during non-hyperthermal stages. The dotted vertical line close to zero is the hyperthermal mean (inverse-variance weighted) RHV across all displayed traits and clades. All error bars show 90% CIs based on variance over six hyperthermal events of the last 300 million years. RHV was calculated using a probabilistic approach (see Section 2). For clarity, clades or traits with  $SE > 2$ , and the much smaller effect size and error of body size, are omitted

### 3.3 | Skeletal mineralogy

Genera with a primary skeletal mineralogy of aragonite had the highest RHV, yielding a 64% chance of raised extinction risk (CIs = 53%–74%; Figures 1 and 2b) over a low-Mg calcite genus. Having a siliceous or low-Mg calcite skeleton was most strongly

associated with genus hyperthermal resistance (Figure 2b). Responses of genera with silica-based skeletons (all sponges) were highly variable at each hyperthermal and had the highest baseline extinction odds of the mineralogic composition categories (Figure S5).

### 3.4 | Motility and life habit

Both actively and facultatively mobile genera had a high RHV, both with 58% (respective CIs = 53%–64% and CIs = 52%–65%) chance of raised extinction risk (Figure 2c). Accordingly, nektonic and infaunal life habits, which strongly overlap these motility groups, also had high RHV (Figure 2d), partly because of very low infaunal baseline extinction odds (Figure S5). Overall, facultatively mobile genera had a significantly higher RHV than stationary genera, but within bivalves this is far from significance (Figure 3b), possibly because most stationary bivalves preferred vulnerable reef habitat (see below; 84% of stationary bivalves with an affinity were for reefs versus 24% of facultatively mobile bivalve genera).

### 3.5 | Body size

In accord with Payne and Heim (2020), we observed decreasing extinction odds with increasing body size within clades, over both hyperthermal and other intervals (Figure S5). However, this selectivity was significantly less pronounced during hyperthermal events than during non-hyperthermal times (Figure 2e). This means that a genus at its clade's third size quartile was more likely to have a raised relative extinction risk (62% chance, CIs = 56%–68%) than a genus at its first quartile. This pattern also held within bivalves (Figure 3d), demonstrating hyperthermal conditions to be linked to a relative decrease in the advantage of a genus having a larger body size.

### 3.6 | Physiological buffering

Fossil clades are often contrasted between those expected to be well-buffered against ambient chemical change and clades characterized by more open, poorly buffered internal chemistry (Bambach et al., 2002). We found that well-buffered genera had lower baseline extinction risk than poorly buffered genera (Figure S5) but did not perform better on average during hyperthermals, with possible exceptions during the PT and early Jurassic hyperthermals (Figure 2f). Examples of well-buffered groups with raised RHV include bony fish and the infaunal trigonid bivalves. A high response variation among poorly buffered genera implies that some organisms within this category, for example, epifaunal bivalve orders Ostreida and Pectinida (Figure 1; also Figure 3c), may be relatively hyperthermal resistant.

**FIGURE 2** Relative hyperthermal vulnerability (RHV) of ecological traits within trait groups, and individual hyperthermal events within traits, accounting for a genus' clade grouping and range size. All error bars show 90% CIs based on variance at hyperthermal events. The dotted vertical lines are the inverse-variance weighted mean RHV across traits within the ecological variable (a–d). The dashed vertical lines are the means of the less vulnerable trait within the ecological variable (f–i). Means of individual hyperthermal events form a time series from the earliest (bottom) to most recent (top; see legend for labels). An equivalent figure for clades is shown in Figure S8. Values are provided in Table S1. Body size is a continuous variable, so panel (e) shows the change in its slope from non-hyperthermal to hyperthermal stages. One value fell far outside the plotting area: Chemosymbiotic RHV at the Paleocene–Eocene Thermal Maximum (PETM) =  $-9.55$  (Table S3)

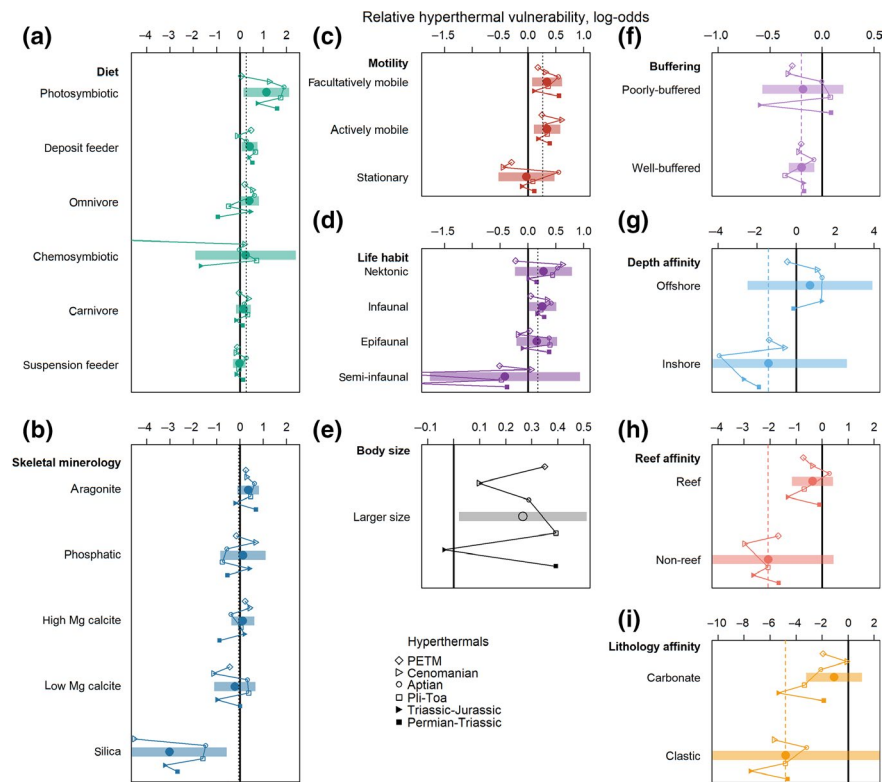
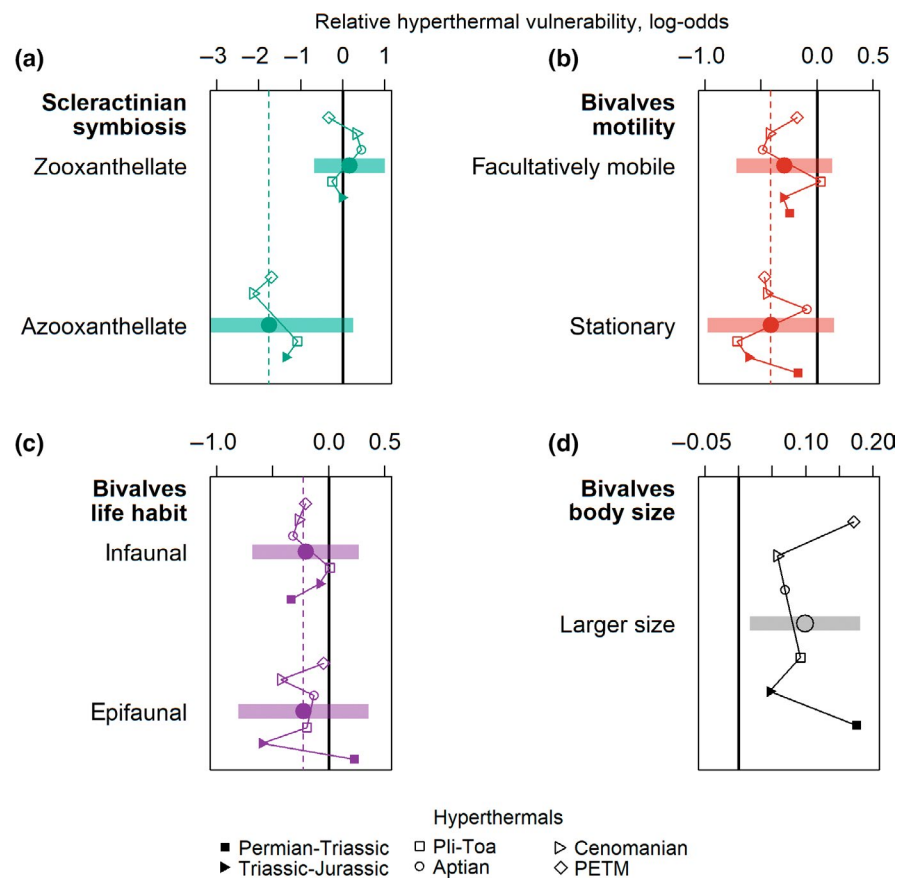


**FIGURE 3** Relative hyperthermal vulnerability (RHV) of traits within clades, accounting for range size. Individual hyperthermal event means are shown within traits using the same scheme and symbols as in Figure 2. Of post-Carboniferous (a) bivalves, 56% are infaunal while 37% are epifaunal; (b) 80% scleractinians are zooxanthellate, the remainder being azooxanthellate; (d) 35% of bivalves are stationary while 64% are facultatively mobile. Note that, while there were 19 survivals, no extinctions of Aptian azooxanthellate corals were observed. All error bars show 90% CIs based on variance at hyperthermal events. The dashed vertical lines are the means of the less vulnerable trait within the ecological variable (a–c). PETM, Paleocene–Eocene Thermal Maximum



### 3.7 | Habitat affinities

Compared against their binary opposites (Figure 2g–i), genera with preferences for reef habitats had a significantly higher RHV than genera preferring non-reef habitats, a rank order that was consistent across different treatments of sampling incompleteness. However, RHV differences between lithology or depth/depositional environment preferences were unclear, the RHV rank order varying by treatment owing to large baseline variation for these genera (Figures S6 and S7).

### 3.8 | Selectivity through time

The early Jurassic hyperthermal (Pli-Toa) was the most selective hyperthermal, whereas vulnerabilities tended to be lowest at the PETM (Figure 2; Figure S8). The investigated hyperthermal events cover both before and after the Middle-Jurassic plankton revolution, which is considered a breakpoint in the buffering capacity of global oceans (Eichenseer et al., 2019) and marks a simultaneous fall in extinction magnitudes of hyperthermal events. Although we wish to know whether selectivity (and thus RHV) patterns changed from before to after the revolution, this is not straightforward due to the rise in selectivity error values that accompanies lower extinction magnitudes (see Methods), alongside the low number of hyperthermals. Therefore, we also checked which traits or clades show decreases in extinction intensity after the Middle Jurassic. As expected, nearly all of the post-revolution changes in hyperthermal extinction selectivity were insignificant (Table S4), but nine out of the 17 “declining selectivity” groups also exhibited a significant drop in extinction intensity (Table S5). This suggests that these groups, including Porifera, genera with low-Mg calcite skeletons, and stationary suspension feeders, became less vulnerable, potentially driving the post-revolution decline in extinction magnitude, although the precise mechanism for this decrease in vulnerability is not clear. Conversely, groups in the top quartile of post-revolution change in extinction selectivity also showed increases in extinction intensity, such as for Actinopterygii, supporting at least a retained post-revolution vulnerability (Table S5).

## 4 | DISCUSSION

We demonstrate that the onset of ancient global warming events systematically increased extinction vulnerability of organisms with particular traits and clade memberships. These traits and clades are therefore candidates for higher-than-usual extinction risk under present-day global warming. The mid-Jurassic plankton revolution may have buffered marine ecosystems against rapid abiotic changes (Eichenseer et al., 2019), thereby decreasing the vulnerability of some groups, but others, including bony fish, likely remain vulnerable to extinction. However, it is difficult to distinguish vulnerability shifts due to this revolution from other gradual changes over time. Modern clades may also exhibit more internal ecological variation

than ancient extinct clades, predominantly because the more ecologically homogenous clades were removed during mass extinctions (Knöpe et al., 2020). This underscores the potential of previous hyperthermals in leading to a general extinction resistance in modern clades, which we also observed as increasing clade response variance over time (Figure S9a), across both baseline and hyperthermal extinctions. For example, stenolaemate bryozoans have extant representatives but several of its orders, such as Trepostomata and Fenestrata, disappeared by the end of the Triassic, potentially leaving surviving genera on average more resistant to extinction (e.g., Cyclostomatida). Thus, Paleozoic and early Mesozoic fossils may overemphasize the vulnerability of some extant groups to global warming. Nevertheless, the rate of modern warming may even exceed rates under ancient hyperthermals (Foster et al., 2017, 2018; but see Kemp et al., 2015), and it is sensible first to crosscheck group vulnerability estimates from fossils with the group's modern performance responses.

Hyperthermal conditions associate with elevated extinction vulnerabilities for photosymbiont hosts (Dunhill et al., 2018). This could arise from difficulties in compromising the needs of both hosts and symbionts under warming-induced stress. For example, rapid rates of heating can increase the production by zooxanthellae of oxygen radicals, which build up within the host coral and can lead to the expulsion of the symbiotic algae, or coral bleaching (e.g., Baird et al., 2018). Repeated mass bleaching threatens populations of photosymbiotic reef builders, such as modern-day scleractinian corals, which can potentially lead to knock-on effects on reef dwellers (Pandolfi et al., 2011). Despite the low extinction magnitude at the most recent hyperthermal, the PETM, a higher RHV of zooxanthellate than azooxanthellate scleractinians aligns with substantial coeval reductions in calcium carbonate production from coral reefs (Kiessling & Simpson, 2011). The key importance of reefs to the spatial configuration of marine biodiversity throughout time (Close et al., 2020; Kiessling et al., 2010) emphasizes the grave potential implications of their vulnerability to global warming.

An increased RHV for deposit feeders, especially at the PETM, is consistent with the PETM being the only extinction event that affected deep-sea foraminifera (Thomas, 2007), which are largely deposit-feeding protists not included in our analysis. Conversely, both foraminifera and bivalve deposit feeders were less affected during the K-Pg hypothermal event (Jablonski & Raup, 1995; Thomas, 2007).

Bony fishes consistently emerged as more relatively vulnerable to hyperthermals than cartilaginous fishes (Vázquez & Clapham, 2017), which remained unchanged following the Jurassic plankton revolution. This distinction is in agreement with a meta-analysis of marine responses to short-term climate-related stressors in modern species (Reddin et al., 2020) and is mirrored by ambivalent range-shift responses of cartilaginous fishes to current climate change in comparison to large shifts by bony fishes (Poloczanska et al., 2013). Other agreements include relative resistance in ostreids, suspension feeders, and taxa with low-Mg calcite skeletons (Reddin et al., 2020), suggesting that short-term performance may scale-up to hyperthermal



survival or extinction (although see next paragraph). For example, rapid temperature rise may promote smaller body sizes in marine ectotherms (Baudron et al., 2014; Peck et al., 2009), which are less likely to exhibit climate-mediated range-shift responses (Kaustuv et al., 2001). Potential mechanisms include a lower risk of oxygen deprivation (Pörtner & Knust, 2007), lower per capita energy needs, faster population responses to change (Genner et al., 2010), and higher abundances than larger body sizes. However, the balancing of ecological advantages and disadvantages over events lasting millennia or longer may be complex.

Our results suggest that, both in ectotherms of the water column and of the benthos, active adult lifestyles incur a relatively elevated risk during hyperthermals compared to outside of hyperthermals. Non-active, stationary lifestyles incur no higher risk at hyperthermals than typical. More active lifestyles enable a higher aerobic scope, the difference between standard and maximum metabolic rate (Bozinovic & Pörtner, 2015; Pörtner et al., 2017), which can confer resistance to acute warming, at least over days to weeks (Peck et al., 2009). Using the activity scheme of Peck et al. (2009) to classify benthic orders and classes, Clapham (2017) observed increased survival odds of genera with higher activity levels during chronic warming at the PT and TJ hyperthermal mass extinctions. However, elevated survival odds for genera with higher activity levels may not be unique to hyperthermals. Following our methods and the activity quotient classifications of Clapham (2017), we support that higher activity values were linked to typically lower extinction odds (non-hyperthermal mean effect size =  $-1.68$ , CIs =  $-1.9$  to  $-1.46$ ). However, this trend is less pronounced during hyperthermals (hyperthermal mean effect size =  $-1.44$ , CIs =  $-1.68$  to  $-1.2$ ), leading to a positive RHV (Figure S9b). Averaged over six hyperthermals, increased RHV suggests that mechanisms of extinction resistance from higher activity rates are less effective at hyperthermals than usual. This reminds that RHV and logistic regression ask different questions: RHV compares the extinction selectivity averages of a group between hyperthermal and non-hyperthermal stages. On the other hand, logistic regression of a single stage calculates the effect of a group on extinction likelihood relative to others for that stage. Separating hyperthermal and non-hyperthermal extinction trends allows RHV to provide additional mechanistic insight. Therefore, the physiological trade-off inherent in an active lifestyle may become less lucrative during hyperthermals. For instance, tolerance of thermal extremes via a larger aerobic scope may give a short-term advantage, but a higher mass-specific basal metabolic rate, demanding more energy and oxygen, might become an increasingly heavy burden when warming-induced seawater hypoxia spreads (Deutsch et al., 2015).

Overlapping with activity levels (Kiessling & Simpson, 2011), physiological buffering categories correlate strongly with extinction rates through the Phanerozoic, leading to a trend in increasing proportions of active and well-buffered genera (Bambach et al., 2002). However, while the underlying mechanisms of

extinction resistance may also be beneficial during hyperthermals, the poorly buffered category obscures a wide range of hyperthermal response successes, indicating diverse tolerance strategies available to these organisms.

Alternative selective pressures can confound clade or trait selectivity, such as latitudinal extinction selectivity. When clades with a high extinction rate are geographical clustered, such as temperate brachiopods during the Changhsingian (Reddin et al., 2019), geographical and clade selectivity are inseparable. However, such issues may be diluted when synthesizing over several stages. Groups that passed our checks against small sample sizes but nevertheless have low ratios of observed to range-through-extrapolated occurrences (i.e., fall to the extreme right of Figure S2, including holothurians, ophiuroids, annelids, and crinoids) should be treated with caution.

## 5 | CONCLUSION

We show that the hypothesis “that the same groups are generally less susceptible to extinction from all possible causes” (McKinney, 1997) neglects that particular biological susceptibilities may be emphasized under global heat stress, which are less relevant under other hypothesized extinction mechanisms such as from competitive interaction or bolide impact (Schulte et al., 2010). Changes in extinction selectivity at ancient hyperthermal events suggest that current climate change may push photosymbiotic scleractinian corals, cohabitants of their reefs, active benthic and nektonic taxa including bony fishes, and larger bodied taxa disproportionately above their typical extinction rates (e.g., Finnegan et al., 2015). Despite the caveats of analyzing fossil responses to hyperthermals, these results show several agreements with rank orders of groups by mean tolerance to modern climate-related stressors in experiments, potentially implicating physiological mechanisms (Reddin et al., 2020). Fossil responses may provide evidence for or against extinction mechanisms under rapid global warming conditions before such extinctions manifest in modern seas.

## ACKNOWLEDGEMENTS

This work was funded by the VolkswagenStiftung and grants from the Deutsche Forschungsgemeinschaft (DFG: AB 109/11-1, KI 806/16-1, and KO 5382/2-1) and is embedded in the Research Unit TERSANE (FOR 2332: Temperature-related stressors as a unifying principle in ancient extinctions). We are sincerely grateful for the constructive reviews of Matthew Clapham and Alex Dunhill that led to an improved manuscript. This work would not be possible without the many PaleoDB data authorizers and enterers, to whom we are truly grateful. This is Paleobiology Database publication number 385. The authors declare to have no conflict of interest. Open access funding enabled and organized by Projekt DEAL.

## DATA AVAILABILITY STATEMENT

The data and R-code that support the main findings of this study are openly available in Dryad at <https://doi.org/10.5061/dryad.qjq2bvqdg>.

## ORCID

Carl J. Reddin  <https://orcid.org/0000-0001-5930-1164>  
 Ádám T. Kocsis  <https://orcid.org/0000-0002-9028-665X>  
 Martin Aberhan  <https://orcid.org/0000-0002-0364-9695>  
 Wolfgang Kiessling  <https://orcid.org/0000-0002-1088-2014>

## REFERENCES

- Aberhan, M., & Baumiller, T. K. (2003). Selective extinction among Early Jurassic bivalves: A consequence of anoxia. *Geology*, 31(12), 1077–1080. <https://doi.org/10.1130/G19938.1>
- Alroy, J. (2008). Dynamics of origination and extinction in the marine fossil record. *Proceedings of the National Academy of Sciences of the United States of America*, 105, 11536–11542. <https://doi.org/10.1073/pnas.0802597105>
- Alroy, J. (2015). A more precise speciation and extinction rate estimator. *Paleobiology*, 41(4), 633–639. <https://doi.org/10.1017/pab.2015.26>
- Baird, M. E., Mongin, M., Rizwi, F., Bay, L. K., Cantin, N. E., Soja-Woźniak, M., & Skerratt, J. (2018). A mechanistic model of coral bleaching due to temperature-mediated light-driven reactive oxygen build-up in zooxanthellae. *Ecological Modelling*, 386, 20–37. <https://doi.org/10.1016/j.ecolmodel.2018.07.013>
- Bambach, R. K., Knoll, A. H., & Sepkoski, J. J. (2002). Anatomical and ecological constraints on Phanerozoic animal diversity in the marine realm. *Proceedings of the National Academy of Sciences of the United States of America*, 99(10), 6854–6859. <https://doi.org/10.1073/pnas.092150999>
- Bates, D., Mächler, M., Bolker, B., & Walker, S. (2015). Fitting linear mixed-effects models using lme4. *Journal of Statistical Software*, 67, 1–48.
- Baudron, A. R., Needle, C. L., Rijnsdorp, A. D., & Tara Marshall, C. (2014). Warming temperatures and smaller body sizes: Synchronous changes in growth of North Sea fishes. *Global Change Biology*, 20(4), 1023–1031. <https://doi.org/10.1111/gcb.12514>
- Bozinovic, F., & Pörtner, H. O. (2015). Physiological ecology meets climate change. *Ecology and Evolution*, 5(5), 1025–1030. <https://doi.org/10.1002/ece3.1403>
- Bush, A. M., Wang, S. C., Payne, J. L., & Heim, N. A. (2020). A framework for the integrated analysis of the magnitude, selectivity, and biotic effects of extinction and origination. *Paleobiology*, 46(1), 1–22. <https://doi.org/10.1017/pab.2019.35>
- Cahill, A. E., Aiello-Lammens, M. E., Fisher-Reid, M. C., Hua, X., Karanewsky, C. J., Yeong Ryu, H., Sbeglia, G. C., Spagnolo, F., Waldron, J. B., Warsi, O., & Wiens, J. J. (2013). How does climate change cause extinction? *Proceedings of the Royal Society B: Biological Sciences*, 280(1750), 20121890.
- Clapham, M. E. (2017). Organism activity levels predict marine invertebrate survival during ancient global change extinctions. *Global Change Biology*, 23, 1477–1485. <https://doi.org/10.1111/gcb.13484>
- Clapham, M. E., & Payne, J. L. (2011). Acidification, anoxia, and extinction: A multiple logistic regression analysis of extinction selectivity during the Middle and Late Permian. *Geology*, 39(11), 1059–1062. <https://doi.org/10.1130/G32230.1>
- Close, R. A., Benson, R. B., Saupe, E. E., Clapham, M. E., & Butler, R. J. (2020). The spatial structure of Phanerozoic marine animal diversity. *Science*, 368(6489), 420–424. <https://doi.org/10.1126/science.aay8309>
- Deutsch, C., Ferrel, A., Seibel, B., Pörtner, H.-O., & Huey, R. (2015). Climate change tightens a metabolic constraint on marine habitats. *Science*, 348(6239), 1132–1136. <https://doi.org/10.1126/science.aaa1605>
- Dunhill, A. M., Foster, W. J., Azaele, S., Sciberras, J., & Twitchett, R. J. (2018). Modelling determinants of extinction across two Mesozoic hyperthermal events. *Proceedings of the Royal Society B: Biological Sciences*, 285, 20180404. <https://doi.org/10.1098/rspb.2018.0404>
- Eichenseer, K., Balthasar, U., Smart, C. W., Stander, J., Haaga, K. A., & Kiessling, W. (2019). Jurassic shift from abiotic to biotic control on marine ecological success. *Nature Geoscience*, 12(8), 638–642. <https://doi.org/10.1038/s41561-019-0392-9>
- Finnegan, S., Anderson, S. C., Harnik, P. G., Simpson, C., Tittensor, D. P., Byrnes, J. E., Finkel, Z. V., Lindberg, D. R., Liow, L. H., Lockwood, R., Lotze, H. K., McClain, C. R., McGuire, J. L., O'Dea, A., & Pandolfi, J. M. (2015). Paleontological baselines for evaluating extinction risk in the modern oceans. *Science*, 348(6234), 567–570. <https://doi.org/10.1126/science.aaa6635>
- Foote, M. (2006). Substrate affinity and diversity dynamics of Paleozoic marine animals. *Paleobiology*, 32(3), 345–366. <https://doi.org/10.1666/05062.1>
- Foote, M., & Raup, D. M. (1996). Fossil preservation and the stratigraphic ranges of taxa. *Paleobiology*, 22, 121–140. <https://doi.org/10.1017/S0094837300016134>
- Foster, G. L., Hull, P., Lunt, D. J., & Zachos, J. C. (2018). Placing our current “hyperthermal” in the context of rapid climate change in our geological past. *Philosophical Transactions. Series A, Mathematical, Physical, and Engineering Sciences*, 376(2130), 20170086. <https://doi.org/10.1098/rsta.2017.0086>
- Foster, G. L., Royer, D. L., Lunt, D. J., Olsen, P. E., & Beerling, D. J. (2017). Future climate forcing potentially without precedent in the last 420 million years. *Nature Communications*, 8, 14845. <https://doi.org/10.1038/ncomms14845>
- Genner, M. J., Sims, D. W., Southward, A. J., Budd, G. C., Masterson, P., Mchugh, M., Rendle, P., Southall, E. J., Wearmouth, V. J., & Hawkins, S. J. (2010). Body size-dependent responses of a marine fish assemblage to climate change and fishing over a century-long scale. *Global Change Biology*, 16(2), 517–527. <https://doi.org/10.1111/j.1365-2486.2009.02027.x>
- Harnik, P. G., Lotze, H. K., Anderson, S. C., Finkel, Z. V., Finnegan, S., Lindberg, D. R., Liow, L. H., Lockwood, R., McClain, C. R., McGuire, J. L., O'Dea, A., Pandolfi, J., Simpson, C., & Tittensor, D. P. (2012). Extinction in ancient and modern seas. *Trends in Ecology & Evolution*, 27(11), 608–617. <https://doi.org/10.1016/j.tree.2012.07.010>
- Harvey, B. P., Gwynn-Jones, D., & Moore, P. J. (2013). Meta-analysis reveals complex marine biological responses to the interactive effects of ocean acidification and warming. *Ecology and Evolution*, 3(4), 1016–1030. <https://doi.org/10.1002/ece3.516>
- Jablonski, D., & Raup, D. M. (1995). Selectivity of end-Cretaceous marine bivalve extinctions. *Science*, 268(5209), 389–391. <https://doi.org/10.1126/science.11536722>
- Kaustuv, R., Jablonski, D., & Valentine, J. W. (2001). Climate change, species range limits and body size in marine bivalves. *Ecology Letters*, 4(4), 366–370. <https://doi.org/10.1046/j.1461-0248.2001.00236.x>
- Kemp, D. B., Eichenseer, K., & Kiessling, W. (2015). Maximum rates of climate change are systematically underestimated in the geological record. *Nature Communications*, 6, 8890. <https://doi.org/10.1038/ncomms9890>
- Kiessling, W., & Aberhan, M. (2007). Environmental determinants of marine benthic biodiversity dynamics through Triassic–Jurassic time. *Paleobiology*, 33(3), 414–434. <https://doi.org/10.1666/06069.1>
- Kiessling, W., & Simpson, C. (2011). On the potential for ocean acidification to be a general cause of ancient reef crises. *Global Change Biology*, 17(1), 56–67. <https://doi.org/10.1111/j.1365-2486.2010.02204.x>
- Kiessling, W., Simpson, C., & Foote, M. (2010). Reefs as cradles of evolution and sources of biodiversity in the Phanerozoic. *Science*, 327(5962), 196–198. <https://doi.org/10.1126/science.1182241>
- Knoll, A. H., Bambach, R. K., Payne, J. L., Pruss, S., & Fischer, W. W. (2007). Paleophysiology and end-Permian mass extinction. *Earth and Planetary Science Letters*, 256(3–4), 295–313. <https://doi.org/10.1016/j.epsl.2007.02.018>
- Knope, M. L., Bush, A. M., Frishkoff, L. O., Heim, N. A., & Payne, J. L. (2020). Ecologically diverse clades dominate the oceans via extinction

- resistance. *Science*, 367(6481), 1035–1038. <https://doi.org/10.1126/science.aax6398>
- Kocsis, Á. T. (2020). *icos*: Global triangular and penta-hexagonal grids based on tessellated icosahedra (R package version 0.10.0.0000). Retrieved from <https://cran.r-project.org/package=icos>
- Kocsis, Á. T., Reddin, C. J., Alroy, J., & Kiessling, W. (2019). The R package divDyn for quantifying diversity dynamics using fossil sampling data. *Methods in Ecology and Evolution*, 10(5), 735–743. <https://doi.org/10.1111/2041-210X.13161>
- McKinney, M. L. (1997). Extinction vulnerability and selectivity: Combining ecological and paleontological views. *Annual Review of Ecology and Systematics*, 28(1), 495–516. <https://doi.org/10.1146/annurev.ecolsys.28.1.495>
- Nürnberg, S., & Aberhan, M. (2015). Interdependence of specialization and biodiversity in Phanerozoic marine invertebrates. *Nature Communications*, 6, 1–8. <https://doi.org/10.1038/ncomms7602>
- Orzechowski, E. A., Lockwood, R., Byrnes, J. E. K., Anderson, S. C., Finnegan, S., Finkel, Z. V., Harnik, P. G., Lindberg, D. R., Liow, L. H., Lotze, H. K., McClain, C. R., McGuire, J. L., O'Dea, A., Pandolfi, J. M., Simpson, C., & Tittensor, D. P. (2015). Marine extinction risk shaped by trait-environment interactions over 500 million years. *Global Change Biology*, 21(10), 3595–3607. <https://doi.org/10.1111/gcb.12963>
- Pandolfi, J. M., Connolly, S. R., Marshall, D. J., & Cohen, A. L. (2011). Projecting coral reef futures under global warming and ocean acidification. *Science*, 333(6041), 418–422. <https://doi.org/10.1126/science.1204794>
- Payne, J. L., & Finnegan, S. (2007). The effect of geographic range on extinction risk during background and mass extinction. *Proceedings of the National Academy of Sciences of the United States of America*, 104(25), 10506–10511. <https://doi.org/10.1073/pnas.0701257104>
- Payne, J. L., & Heim, N. A. (2020). Body size, sampling completeness, and extinction risk in the marine fossil record. *Paleobiology*, 46(1), 23–40. <https://doi.org/10.1017/pab.2019.43>
- Peck, L. S., Clark, M. S., Morley, S. A., Massey, A., & Rossetti, H. (2009). Animal temperature limits and ecological relevance: Effects of size, activity and rates of change. *Functional Ecology*, 23(2), 248–256. <https://doi.org/10.1111/j.1365-2435.2008.01537.x>
- Piazza, V., Ullmann, C. V., & Aberhan, M. (2020). Temperature-related body size change of marine benthic macroinvertebrates across the Early Toarcian Anoxic Event. *Scientific Reports*, 10(1), 1–13. <https://doi.org/10.1038/s41598-020-61393-5>
- Poloczanska, E. S., Brown, C. J., Sydeman, W. J., Kiessling, W., Schoeman, D. S., Moore, P. J., Brander, K., Bruno, J. F., Buckley, L. B., Burrows, M. T., Duarte, C. M., Halpern, B. S., Holding, J., Kappel, C. V., O'Connor, M. I., Pandolfi, J. M., Parmesan, C., Schwing, F., Thompson, S. A., & Richardson, A. J. (2013). Global imprint of climate change on marine life. *Nature Climate Change*, 3(10), 919–925. <https://doi.org/10.1038/nclimate1958>
- Pörtner, H.-O., Bock, C., & Mark, F. C. (2017). Oxygen- and capacity-limited thermal tolerance: Bridging ecology and physiology. *Journal of Experimental Biology*, 220, 2685–2696. <https://doi.org/10.1242/jeb.134585>
- Pörtner, H.-O., & Knust, R. (2007). Climate change affects marine fishes through the oxygen limitation of thermal tolerance. *Science*, 315, 95–98. <https://doi.org/10.1126/science.1135471>
- Raup, D. M., & Boyajian, G. E. (1988). Patterns of generic extinction in the fossil record patterns of generic extinction in the fossil record. *Paleobiology*, 14(2), 109–125. <https://doi.org/10.1017/S009483730011866>
- Reddin, C. J., Kocsis, Á. T., & Kiessling, W. (2019). Climate change and the latitudinal selectivity of ancient marine extinctions. *Paleobiology*, 45, 70–84. <https://doi.org/10.1017/pab.2018.34>
- Reddin, C. J., Nätscher, P. N., Kocsis, Á. T., Pörtner, H. O., & Kiessling, W. (2020). Marine clade sensitivities to climate change conform across time scales. *Nature Climate Change*, 10, 249–253. <https://doi.org/10.1038/s41558-020-0690-7>
- Ridgwell, A. (2005). A mid Mesozoic Revolution in the regulation of ocean chemistry. *Marine Geology*, 217(3–4), 339–357. <https://doi.org/10.1016/j.margeo.2004.10.036>
- Schulte, P., Alegret, L., Arenillas, I., Arz, J. A., Barton, P. J., Bown, P. R., Bralower, T. J., Christeson, G. L., Claeys, P., Cockell, C. S., Collins, G. S., Deutsch, A., Goldin, T. J., Goto, K., Grajales-Nishimura, J. M., Grieve, R. A. F., Gulick, S. P. S., Johnson, K. R., Kiessling, W., ... Willumsen, P. S. (2010). The Chicxulub asteroid impact and mass extinction at the Cretaceous-Paleogene boundary. *Science*, 327(5970), 1214–1218. <https://doi.org/10.1126/science.1177265>
- Storch, D., Menzel, L., Frickenhaus, S., & Pörtner, H. O. (2014). Climate sensitivity across marine domains of life: Limits to evolutionary adaptation shape species interactions. *Global Change Biology*, 20(10), 3059–3067. <https://doi.org/10.1111/gcb.12645>
- Suan, G., Mattioli, E., Pittet, B., Lécuyer, C., Suchéras-Marx, B., Duarte, L. V., Philippe, M., Reggiani, L., & Martineau, F. (2010). Secular environmental precursors to Early Toarcian (Jurassic) extreme climate changes. *Earth and Planetary Science Letters*, 290(3–4), 448–458. <https://doi.org/10.1016/j.epsl.2009.12.047>
- Sun, Y., Joachimski, M. M., Wignall, P. B., Yan, C., Chen, Y., Jiang, H., Wang, L., & Lai, X. (2012). Lethally hot temperatures during the Early Triassic greenhouse. *Science*, 338, 366–370. <https://doi.org/10.1126/science.1224126>
- Thomas, E. (2007). Cenozoic mass extinctions in the deep sea; what disturbs the largest habitat on Earth? In S. Monechi, R. Coccioni, & M. Rampino (Eds.), *Large ecosystem perturbations: Causes and consequences*. Geological Society of America special paper (Vol. 424, pp. 1–24). The Geological Society of America, Inc.
- van Buuren, S., & Groothuis-Oudshoorn, K. (2011). mice: Multivariate imputation by chained equations in R. *Journal of Statistical Software*, 45, 1–67. <https://doi.org/10.18637/jss.v045.i03>
- Vázquez, P., & Clapham, M. E. (2017). Extinction selectivity among marine fishes during multistressor global change in the end-Permian and end-Triassic crises. *Geology*, 45, 395–398. <https://doi.org/10.1130/G38531.1>
- Viechtbauer, W. (2010). Conducting meta-analyses in R with the metafor package. *Journal of Statistical Software*, 36, 1–48.
- Wittmann, A. C., & Pörtner, H. O. (2013). Sensitivities of extant animal taxa to ocean acidification. *Nature Climate Change*, 3(11), 995–1001. <https://doi.org/10.1038/nclimate1982>

## SUPPORTING INFORMATION

Additional supporting information may be found online in the Supporting Information section.

**How to cite this article:** Reddin CJ, Kocsis ÁT, Aberhan M, Kiessling W. Victims of ancient hyperthermal events herald the fates of marine clades and traits under global warming. *Glob Change Biol*. 2020;00:1–11. <https://doi.org/10.1111/gcb.15434>